Flexibility Management in Economic Dispatch With Dynamic Automatic Generation Control

Lei Fan, *Senior Member, IEEE*, Chaoyue Zhao, *Member, IEEE*, Guangyuan Zhang, *Member, IEEE*, and Qiuhua Huang, *Member, IEEE*

***Abstract*—As the installation of electronically interconnected renewable energy resources grows rapidly in power systems, system frequency maintenance and control become challenging problems to maintain the system reliability in bulk power systems. As two of the most important frequency control actions in the control centers of independent system operators (ISOs) and utilities, the interaction between Economic Dispatch (ED) and Automatic Generation Control (AGC) attracts more and more attention. In this paper, we propose a robust optimization based framework to measure the system flexibility by considering the interaction between two hierarchical processes (i.e., ED and AGC). We propose a cutting plane algorithm with the reformulation technique to obtain seven different indices of the system. In addition, we study the impacts of several system factors (i.e., the budget of operational cost, ramping capability, and transmission line capacity) and show numerically how these factors can influence the system flexibility.**

***Index Terms*—Economic dispatch, automatic generation control (AGC), flexibility management, robust optimization, cutting plane method.**

NOMENCLATURE

A. Sets

$\mathcal{B}$	Set of buses.
$\mathcal{G}$	Set of generators.
$\mathcal{G}^b$	Set of generators at bus b.
$\mathcal{L}$	Set of transmission lines.

B. Parameters

CP_n	Penalty cost for generator n in dynamic AGC constraints.
τ	Budget for the total operational cost.
C^{REGU_n}	Regulation up cost for generator n.
C^{REGD_n}	Regulation down cost for generator n.
C^{SR_n}	Spinning reserve cost for generator n.
F_l	Transmission capacity of transmission line l (MW).
$\text{P}_n^{\max}$	Maximum generation amount (MW) of generator n.
$\text{P}_n^{\min}$	Minimum generation amount (MW) of generator n.
REG_n^{U}	Maximum regulation up amount of generator n.
REG^{MinU}	Minimum regulation up requirement of the system.
REG_n^{D}	Maximum regulation down amount of generator n.
REG^{MinD}	Minimum regulation down requirement of the system.
$\text{SR}_n^{\max}$	Maximum spinning reserve amount of generator n.
$\text{SR}^{\min}$	Minimum spinning reserve requirement of the system.
RUR_n	Maximum ramping up rate of generator n.
RDR_n	Maximum ramping down rate of generator n.
$\text{SF}_{b,l}$	Shift factors of transmission line l and bus b.
$\bar{d}_b$	Nominal load amount at bus b.
$\Delta\bar{d}_t$	Nominal system load change amount at sub time interval t.
$\hat{d}_b$	The maximum deviation amount from nominal load amount at bus b.
$\Delta\hat{d}_t$	The maximum load disturbance amount from the nominal value at sub time interval t.
$\Delta\omega_t^{\min}$	Minimum system frequency change at sub time interval t.
$\Delta\omega_t^{\max}$	Maximum system frequency change at sub time interval t.

C. Random Parameters

d_b	Random load on bus b (MW).
Δd_t	Random system load disturbance (MW) at sub time interval t.

D. Decision Variables

oc_n	Generation cost function of generator n.
λ_b^{up}	The scale of upper deviation of load at bus b.
λ_b^{dn}	The scale of lower deviation of load at bus b.
λ_t^{up}	The scale of upper deviation of system load within one sub time interval t.
λ_t^{dn}	The scale of lower deviation of system load within one sub time interval t.
p_n	Generation amount of generator n (MW).
$\Delta f_{n,t}^{\text{AGC}+}$	Slack variable for dynamic AGC constraints for generator n at sub time interval t.
$\Delta f_{n,t}^{\text{AGC}-}$	Slack variable for dynamic AGC constraints for generator n at sub time interval t.
reg_n^{U}	Regulation up amount of generator n (MW).

Manuscript received June 5, 2020; revised November 24, 2020 and March 30, 2021; accepted July 11, 2021. Date of publication August 10, 2021; date of current version March 28, 2022. This work was supported by National Science Foundation (NSF) under Grants 2045978 and 2046243. Paper no. TPWRS-00932-2020. *(Corresponding author: Chaoyue Zhao.)*

Lei Fan is with the Department of Engineering Technology, University of Houston, Houston, TX 77204 USA (e-mail: lfan8@central.uh.edu).

Chaoyue Zhao is with the Department of Industrial and Systems Engineering, University of Washington at Seattle, Seattle, WA USA (e-mail: cyzhao@uw.edu).

Guangyuan Zhang is with RWE Renewables, Austin, TX 78701 USA (e-mail: zhangguangyuan1985@gmail.com).

Qiuhua Huang is with the Pacific Northwest National Laboratory, Richland, WA 99352 USA (e-mail: qiuhua.huang@pnnl.gov).

Color versions of one or more figures in this article are available at https://doi.org/10.1109/TPWRS.2021.3103128.

Digital Object Identifier 10.1109/TPWRS.2021.3103128

reg_n^{D} Regulation down amount of generator n (MW).
sr_n Spinning reserve of generator n (MW).
$\Delta p_{n,t}^{\mathrm{REF}}$ The reference AGC signal for generator n at sub time interval t.
$\Delta p_{n,t}^{\mathrm{M}}$ The prime power generation change of generator n at sub time interval t.
$\Delta \omega_t$ System frequency change.

I. Introduction

AS THE 3D (decarbonization, digitization and decentralization) trend becomes the mainstream in the evolution of energy systems, more and more renewable energy resources are installed in the bulk power systems. For example, as projected by U.S. Energy Information Administration (EIA) [1], the total share of electricity generation from the renewable energy will be 38% by 2050. In particular, solar energy and wind energy will contribute 17.5% and 12.54% of the total electricity generation by 2050 respectively. Moreover, New York state plans to reach 100% carbon-free by 2050 [2], and California state sets its 100% clean electric power goal by 2045 [3]. The increase of these carbon-free and non-dispatchable energy resources requires the enhancement of the digital management capability of ISOs and utilities.

In order to hedge against the variability and uncertainty of renewable energy generation and therefore achieve a high penetration of renewable energy to the power system, the concept of flexibility has been proposed and investigated, to gauge the capability of the power system in addressing the variability of the net demand (demand net of wind and solar) [4], [5]. From the time scale's perspective, the flexibilities on planning and operations of the power system have been recently investigated. For example, the index of insufficient ramping resource expectation (IRRE) is proposed in [6] to reflect the flexibility of the power system in the generation expansion planning. Operational flexibility and local flexibility for the power system operated by transmission system operators are discussed in [7]. From market design's perspective, ISOs developed different commodity products for the electricity market to capture the flexibility of the resources. For example, CAISO and MISO developed market-based flexible ramping products that can improve the availability of the system's ramping capacity [8]. ERCOT designed a fast frequency response product to maintain sufficient primary frequency control capability under a high penetration of renewable energy [9]. In addition, MISO is investigating short-term reserve products to enhance the system flexibility and ensure reserve deliverability [10]. All these new market designs effectively provide the pricing signal to flexible resources in the energy market system. On the resource level, researchers have investigated flexible generation resources such as combined-cycle power plants [11] and [12], pump-storage plants [13], battery energy storage [14] and [15]. These complex operation models of multi-cycle or multi-stage energy resources in the electricity market not only can strengthen the capability of the grid to respond to the dynamic change of net demand, but also can reduce the operational cost of the electricity grid [16]. In addition, the modeling approaches for aggregations of flexible resources such as virtual power plants and distributed energy resources aggregators have also been studied in [17] and [18].

In this paper, we focus on the flexibility of the power system, motivated by the flexibility metric framework proposed by the researchers from ISO-NE [19]. In [19], the system flexibility is measured in four dimensions (i.e., time, action, uncertainty, and cost). In the time dimension, the short-term flexibility indicates the capability of the system in responding to emergencies or contingencies from minutes to hours. The long-term flexibility indicates the capability of the system in adapting the change of the generation portfolio, system topology, and regulator policy. In the action dimension, different control schemes (e.g., automatic generation control, economic dispatch, unit commitment, outage management, generation and transmission expansion) can be taken by system operators based on different response time windows to address the variability of the net demand. In the uncertainty dimension, system operators need to manage resources to tackle randomnesses such as equipment failures or forecasting errors of the net demand. Then, the cost restricts the availability of control schemes. With these, the overall system flexibility of the economic dispatch under the uncertainty can be calculated in a systematic way, and the problem can be reformulated as a classic two-stage robust optimization model [20], [21], and [22].

In the current electricity market practice, ED, which usually runs every 5 minutes, provides generation resources with the base dispatch point and regulation reserve capacity [23], [24], and [25]. However, the traditional ED process does not consider the impact of dynamic AGC, which is executed every 2–6 seconds, with the objective of maintaining the system frequency. This conventional ED-AGC hierarchical model may not be able to provide sufficient system flexibility under a high renewable penetration to track the second-to-second net demand variation [26] and [27]. Therefore, we will study the flexibility management by explicitly considering the interaction between ED and the dynamic AGC.

The contributions of our paper can be summarized as follows.

1) We propose a robust optimization based framework to measure the system flexibility of the dynamic AGC constrained economic dispatch process. Then, we develop a separation framework to effectively solve the robust feasibility problem.
2) We propose seven flexibility indices for a systematic evaluation of the system flexibility, and analyze the system characteristics by using the flexibility management tool to help the system operator understand the impacts of multiple system factors (e.g., budget, ramping capability, and transmission line capability) on the system flexibility.

We organize the remaining part of this paper as follows. Section II describes the mathematical formulation of the system's flexibility based on the AGC constrained economic dispatch. Section IV reports the studies of flexibility in IEEE standard systems. Section V concludes the findings of our paper.

II. Mathematical Formulation of Flexibility

In this section, we deploy a robust optimization based framework to measure the system flexibility of the economic dispatch with the dynamic AGC. In current practice, within every 5-minute interval ED run, the system frequency is adjusted by AGC to its nominal value for every 2–6 seconds. In this paper, we consider the system dynamics within an ED run cycle, i.e., 5 minutes. That is, the overall time horizon is set to be 5 minutes. Within the ED cycle, we consider all the AGC cycles as a set of time interval $\mathcal{T}$. Both load at each bus and system load disturbance in each time period are assumed to be random and are within an undetermined variation range. That is,

$$d_b \in \mathcal{U}_b(\lambda) = [\bar{d}_b - \lambda_b^{dn}\hat{d}_b, \bar{d}_b + \lambda_b^{up}\hat{d}_b], \ \ \forall b \in \mathcal{B}$$

and

$$\Delta d_t \in \mathcal{U}_t(\lambda) = [\Delta\bar{d}_t - \lambda_t^{dn}\Delta\hat{d}_t, \Delta\bar{d}_t + \lambda_t^{up}\Delta\hat{d}_t], \ \ \forall t \in \mathcal{T},$$

where $\bar{d}_b$ and $\hat{d}_b$ represent the nominal value and maximum deviation of the load at bus b in the economic dispatch, and $\Delta\bar{d}_t$ and $\Delta\hat{d}_t$ represent the nominal value and maximum deviation of the system load disturbances at each AGC cycle time period t. Notice that the load change on each bus in the economic dispatch is an average value in the five minutes economic dispatch cycle. In the 2–4 second AGC cycle, the system operator use system load disturbances to capture the dynamic process of the system load. $\lambda_{\{b,t\}}^{\{up,dn\}} \in [0,1]$ represent the scales of the deviation for the corresponding variation range. Unlike the traditional robust optimization model that the size of the uncertainty set is predefined, in our model, we will obtain the largest size of each uncertainty set by deciding the scales $\lambda_{\{b,t\}}^{\{up,dn\}}$, to measure the system flexibility that the system can accommodate.

Based on the economic dispatch with dynamic AGC model proposed by [27], we develop a flexibility measurement model as described in Section II-A.

A. Formulation

$$\max \ \sum_{b\in\mathcal{B}}(\hat{d}_b\lambda_b^{up} + \hat{d}_b\lambda_b^{dn}) + \sum_{t\in\mathcal{T}}(\Delta\hat{d}_t\lambda_t^{up} + \Delta\hat{d}_t\lambda_t^{dn}) \quad (1a)$$

$$\text{s.t.} \sum_{n\in\mathcal{G}} \big(oc_n(p_n) + C^{\text{REGU}_n} reg_n^{\text{U}} + C^{\text{REGD}_n} reg_n^{\text{D}} + C_n^{\text{SR}} sr_n\big) + \sum_{t\in\mathcal{T}} \text{CP}_n \Delta f_t^{\text{AGC+}} + \sum_{t\in\mathcal{T}} \text{CP}_n \Delta f_t^{\text{AGC}-} \le \tau \quad (1b)$$

$$p_n + reg_n^{\text{U}} + sr_n \le \text{P}_n^{\max}, \forall n \in \mathcal{G}, \quad (1c)$$

$$\text{P}_n^{\min} \le p_n - reg_n^{\text{D}}, \forall n \in \mathcal{G}, \quad (1d)$$

$$reg_n^{\text{U}} \le \text{REG}_n^{\text{U}}, \forall n \in \mathcal{G}, \quad (1e)$$

$$reg_n^{\text{D}} \le \text{REG}_n^{\text{D}}, \forall n \in \mathcal{G}, \quad (1f)$$

$$sr_n \le \text{SR}_n^{\max}, \forall n \in \mathcal{G}, \quad (1g)$$

$$P_n^0 - p_n \le \text{RDR} \quad (1h)$$

$$p_n - P_n^0 \le \text{RUR} \quad (1i)$$

$$\Delta p_{n,t+1}^{\text{M}} = \sum_{i\in\mathcal{G}}(\alpha_{i,n}\Delta p_{i,t}^{\text{M}} + \beta_{i,n}\Delta p_{i,t}^{\text{REF}}) + \gamma_n\Delta\omega_t + \zeta_n\Delta d_t, \forall n \in \mathcal{G}, \forall \Delta d_t \in \mathcal{U}_t, \forall t \in \mathcal{T}, \quad (1j)$$

$$\Delta\omega_{t+1} = \sum_{i\in\mathcal{G}}(\kappa_i\Delta p_{i,t}^{\text{M}} + \tau_i\Delta p_{i,t}^{\text{REF}}) + \rho\Delta\omega_t + \eta\Delta d_t, \forall \Delta d_t \in \mathcal{U}_t, \forall t \in \mathcal{T}, \quad (1k)$$

$$\sum_{n\in\mathcal{G}}(\Delta p_{n,t+1}^{\text{REF}} - \Delta p_{n,t}^{\text{REF}}) + \Delta f_{t+1}^{\text{AGC+}} - \Delta f_{t+1}^{\text{AGC}-} = K\Delta\omega_{t+1}, \forall t \in \mathcal{T} \quad (1l)$$

$$\Delta p_{n,t+1}^{\text{M}} - \Delta p_{n,t}^{\text{M}} \le \text{RUR}_n, \forall n \in \mathcal{G}, \forall t \in \mathcal{T} \quad (1m)$$

$$\Delta p_{n,t}^{\text{M}} - \Delta p_{n,t+1}^{\text{M}} \le \text{RDR}_n, \forall n \in \mathcal{G}, \forall t \in \mathcal{T} \quad (1n)$$

$$-reg_n^{\text{D}} \le \Delta p_{n,t}^{\text{REF}} \le reg_n^{\text{U}}, \forall n \in \mathcal{G}, \forall t \in \mathcal{T} \quad (1o)$$

$$\Delta\omega^{\min} \le \Delta\omega_t \le \Delta\omega^{\max}, \forall t \in \mathcal{T} \quad (1p)$$

$$\sum_{n\in\mathcal{G}} p_n - \sum_{b\in\mathcal{B}} d_b = 0, \forall d_b \in \mathcal{U}_b, \quad (1q)$$

$$\sum_{n\in\mathcal{G}} sr_n \ge \text{SR}^{\min}, \quad (1r)$$

$$\sum_{n\in\mathcal{G}} reg_n^{\text{U}} \ge \text{REG}^{\text{MinU}}, \quad (1s)$$

$$\sum_{n\in\mathcal{G}} reg_n^{\text{D}} \ge \text{REG}^{\text{MinD}}, \quad (1t)$$

$$-F_l \le \sum_{b\in\mathcal{B}} \text{SF}_{b,l}\Big(\sum_{n\in\mathcal{G}^b} p_n - d_b\Big) \le F_l, \forall d_b \in \mathcal{U}_b, \quad (1u)$$

$$p_n, reg_n^{\text{U}}, reg_n^{\text{D}}, sr_n, \Delta f_t^{\text{AGC+}}, \Delta f_t^{\text{AGC}-} \ge 0,$$
$$\Delta p_{n,t}^{\text{REF}}, \Delta p_{n,t}^{\text{M}}, \Delta\omega_t \text{ free},$$
$$\lambda_b^{up}, \lambda_b^{dn}, \lambda_t^{up}, \lambda_t^{dn} \in [0,1], \forall b \in \mathcal{B}, \forall n \in \mathcal{G}, \forall t \in \mathcal{T}, \quad (1v)$$

where the objective function is to maximize the variation range of the uncertainty. This model has the decision variables including p_n, reg_n^{U}, reg_n^{D}, sr_n, $\Delta f_t^{\text{AGC+}}$, $\Delta f_t^{\text{AGC}-}$, $\Delta p_{n,t}^{\text{REF}}$, $\Delta p_{n,t}^{\text{M}}$, $\Delta\omega_t$, λ_b^{up}, λ_b^{dn}, λ_t^{up}, λ_t^{dn}. Constraints (1b) represent the budget constraint, which indicates that the total fuel cost and the penalty cost should not exceed a budget τ. Constraints (1c) and (1d) represent the generation limits of traditional thermal units that take account of generation output, regulation and spinning reserves. Constraints (1e)–(1i) represent the capacities for providing regulation up, regulation down, spinning reserve services, ramping up/down, respectively. Constraints (1j)–(1l) represent AGC dynamic system constraints, i.,e., the transformation of state vectors $\Delta p_{n,t}^{\text{M}}$, $\Delta p_{n,t}^{\text{REF}}$, $\Delta\omega_t$ from t to $t+1$ given

any demand disturbance Δd_t, where the matrix components $\alpha, \beta, \gamma, \zeta, \kappa, \tau, \rho, \eta$ can be calculated by numerous methods such as zero-order hold method [27]. Constraints (1m) and (1n) restrict ramping up and ramping down limits. Constraints (1o) indicate that the governor generation change should not exceed the regulation service reserved, and constraints (1p) restrict the limit of system frequency change. In addition, the power balance constraints are described in (1q), which should be held for any load realization within the uncertainty set; constraints (1r)–(1t) describe the overall spinning reserve, regulation up, and regulation down requirements respectively, and constraints (1u) represent the transmission capacity constraints.

B. Solution Methodology

First, for notation brevity, we use matrices and vectors to represent constraints and variables, and rewrite the above model in an abstract compact form (denoted as ACF):

$$(\text{ACF}) \quad \max \ a^T\lambda \tag{2a}$$

$$\text{s.t.} \ \ A_1 x \le b_1, \tag{2b}$$

$$A_2 x = H_2 d, \ \ \forall d_b \in \mathcal{U}_b(\lambda), \forall b \in \mathcal{B}, \tag{2c}$$

$$A_3 x \le H_3 d, \ \ \forall d_b \in \mathcal{U}_b(\lambda), \forall b \in \mathcal{B}, \tag{2d}$$

$$A_4 y = H_4 \Delta d, \ \ \Delta d_t \in \mathcal{U}_t(\lambda), \forall t \in \mathcal{T}, \tag{2e}$$

$$A_5 y = b_5, \tag{2f}$$

$$A_6 y \le b_6, \tag{2g}$$

$$A_7 x + A_8 y \le b_7, \tag{2h}$$

where $x = (p, reg^{\text{U}}, reg^{\text{D}}, sr)$, $y = (\Delta p^{\text{M}}, \ \Delta p^{\text{REF}}, \ \Delta\omega, \Delta f^{\text{AGC}+}, \Delta f^{\text{AGC}-})$, $d = (d_1, \ldots, d_b, \cdots)_{b\in\mathcal{B}}$, and $\Delta d = (\Delta d_1, \cdots, \Delta d_t, \cdots)_{t\in\mathcal{T}}$; objective (2a) represents (1a); constraint (2b) represents (1c)–(1i) and (1r)–(1t); constraint (2c) represents (1q); constraint (2d) represents (1u); constraint (2e) represents (1j) and (1k); constraint (2f) represents (1l); constraint (2g) represents (1m), (1n), and (1p); constraint (2h) represents (1b) and (1o).

We deploy cutting plane method to solve the problem. Since the problem is to find the largest deviation of the uncertainty set that the system can accommodate, i.e., the largest value of λ without making the constraints (2b)–(2h) infeasible, therefore, only feasibility cuts are needed.

1) Master Problem and Subproblem: We first decompose problem ACF into a master problem (denoted as MAP) and a subproblem.

$$(\text{MAP}) \ \max \ a^T\lambda \tag{3a}$$

$$\text{s.t.} \ g(\lambda) \le 0 \tag{3b}$$

$$\mathbf{0} \le \lambda \le \mathbf{1} \tag{3c}$$

Here, the feasibility cuts are represented in (3b), and $\mathbf{0}$, $\mathbf{1}$ represent vectors with all components 0 and 1 respectively At the beginning of the iterations, the λ, generated by solving the master problem, makes the subproblem (4a) infeasible. The feasibility cuts in (3b) can help cut off these points (i.e., λ). To generate the feasibility cuts, we first describe the feasibility check problem (denoted as FEA) as follows:

$$(\text{FEA}) \max_{d_b\in\mathcal{U}_b, \Delta d_t\in\mathcal{U}_t} \min_{x,y,s} \ \mathbf{1}^T s \tag{4a}$$

$$\text{s.t.} \ \ A_1 x - s_1 \le b_1, \tag{4b}$$

$$A_2 x + s_2^+ - s_2^- = H_2 d, \tag{4c}$$

$$A_3 x - s_3 \le H_3 d, \tag{4d}$$

$$A_4 y + s_4^+ - s_4^- = H_4 \Delta d, \tag{4e}$$

$$A_5 y + s_5^+ - s_5^- = b_5, \tag{4f}$$

$$A_6 y - s_6 \le b_6, \tag{4g}$$

$$A_7 x + A_8 y - s_7 \le b_7. \tag{4h}$$

If λ is feasible, then the optimal value of (FEA) will be 0.

2) Reformulation of Subproblem: Now we take the dual of the inner minimization of subproblem (FEA) and combine the dual problem with the outer maximization problem, then we can get the following formulation:

$$(\text{DFEA}) \max_{d_b\in\mathcal{U}_b, \Delta d_t\in\mathcal{U}_t, \mu} \ b_1^T\mu_1 + d^T H_2^T\mu_2 + d^T H_3^T\mu_3 + \Delta d^T H_4^T\mu_4 + b_5^T\mu_5 + b_6^T\mu_6 + b_7^T\mu_7 \tag{5a}$$

$$\text{s.t.} \ A_1^T\mu_1 + A_2^T\mu_2 + A_3^T\mu_3 + A_7^T\mu_7 \le 0, \tag{5b}$$

$$A_4^T\mu_4 + A_5^T\mu_5 + A_6^T\mu_6 + A_8^T\mu_7 = 0, \tag{5c}$$

$$-\mathbf{1} \le \mu_k \le \mathbf{0}, \forall k \in \{1, 3, 6, 7\} \tag{5d}$$

$$-\mathbf{1} \le \mu_k \le \mathbf{1}, \forall k \in \{2, 4, 5\}, \tag{5e}$$

where $\mu_1, \mu_2, \mu_3, \mu_4, \mu_5, \mu_6, \mu_7$ are dual variables for constraints (4b)–(4h) respectively.

In the above formulation (DFEA), we have bilinear terms $d^T H_2^T\mu_2$, $d^T H_3^T\mu_3$, and $\Delta d^T H_4^T\mu_4$. We will deal with $d^T H_3^T\mu_3$ first. Let N_i represent the dimension of μ_i and λ^* represent the optimal solution of problem (MAP). Based on the property of d, $\forall b \in \mathcal{B}$, we can rewrite it as $d_b = \bar{d}_b + z_b^+\lambda_b^{*,up}\hat{d}_b - z_b^-\lambda_b^{*,dn}\hat{d}_b$. Here we introduce two binary variables z_b^+ and z_b^- to indicate the deviation direction. Note that the variables $\lambda^{*,up}$ and $\lambda^{*,dn}$ have been fixed for DFEA problem. Therefore, we can replace the bilinear term $d^T H_3^T\mu_3$ as follows:

$$\begin{aligned} d^T H_3^T\mu_3 &= \sum_{b\in\mathcal{B}}\sum_{i=1}^{N_3} d_b H_{3,i,b}\mu_{3,i} \\ &= \sum_{b\in\mathcal{B}}\sum_{i=1}^{N_3} (\bar{d}_b H_{3,i,b}\mu_{3,i} + \lambda_b^{*,up}\hat{d}_b H_{3,i,b} z_b^+\mu_{3,i} \\ &\quad - \lambda_b^{*,dn}\hat{d}_b H_{3,i,b} z_b^-\mu_{3,i}) \end{aligned} \tag{6a}$$

$$z_b^+ + z_b^- = 1, z_b^+, z_b^- \in \{0, 1\} \tag{6b}$$

In (6a), we have two bilinear items $z_b^+\mu_{3,i}$ and $z_b^-\mu_{3,i}$, which can be further linearized by introducing auxiliary variables $\mu_{3,b,i}^+$ and $\mu_{3,b,i}^-$. By following the approach indicated in [28], we have

the following reformulation which is equivalent to (6a):

$$d^T H_3^T \mu_3 = \sum_{b\in\mathcal{B}}\sum_{i=1}^{N_3}(\bar{d}_b H_{3,i,b}\mu_{3,i} + \lambda_b^{*,up}\hat{d}_b H_{3,i,b}\mu_{3,b,i}^{+} - \lambda_b^{*,dn}\hat{d}_b H_{3,i,b}\mu_{3,b,i}^{-}) \quad (7a)$$

$$-z_b^{+} \le \mu_{3,b,i}^{+},\ \mu_{3,i} \le \mu_{3,b,i}^{+} \le 1 - z_b^{+} + \mu_{3,i}, \quad (7b)$$

$$-z_b^{-} \le \mu_{3,b,i}^{-},\ \mu_{3,i} \le \mu_{3,b,i}^{-} \le 1 - z_b^{-} + \mu_{3,i}, \quad (7c)$$

$$z_b^{+} + z_b^{-} = 1, z_b^{+}, z_b^{-} \in \{0,1\}, \quad (7d)$$

$$-1 \le \mu_{3,b,i}^{+} \le 0, \forall b \in \mathcal{B}, \forall i = 1,\dots,N_3. \quad (7e)$$

$$-1 \le \mu_{3,b,i}^{-} \le 0, \forall b \in \mathcal{B}, \forall i = 1,\dots,N_3. \quad (7f)$$

For $d^T H_2^T \mu_2$ and $\Delta d^T H_4^T \mu_4$, we can use a similar approach. We will use $d^T H_2^T \mu_2$ as an example and the other follows the same approach. Since $\mu_2 \in [-\mathbf{1}, \mathbf{1}]$, we can replace it with $\mu_2^n - \mu_2^p$ and $-\mathbf{1} \le \mu_2^n \le \mathbf{0}$ and $-\mathbf{1} \le \mu_2^p \le \mathbf{0}$. Then $d^T H_2^T \mu_2 = d^T H_2^T \mu_2^n - d^T H_2^T \mu_2^p$. For $d^T H_2^T \mu_2^n$ and $d^T H_2^T \mu_2^p$, we will follow the same procedure of (7a)–(7f) to linearize them. Therefore, we can reformulate the (DEFA) problem as follows:

$$\begin{aligned}(\text{RDFEA}) \max_{d_b,\Delta d_t,\mu}\ & b_1^T\mu_1 + \sum_{b\in\mathcal{B}}\sum_{i=1}^{N_2}\{\bar{d}_b H_{2,i,b}(\mu_{2,i}^n - \mu_{2,i}^p) \\ &+\lambda_b^{*,up}\hat{d}_b H_{2,i,b}(\mu_{2,b,i}^{n,+} - \mu_{2,b,i}^{p,+}) - \lambda_b^{*,dn}\hat{d}_b H_{2,i,b}(\mu_{2,b,i}^{n,-} - \mu_{2,b,i}^{p,-})\} \\ &+ \sum_{b\in\mathcal{B}}\sum_{i=1}^{N_3}(\bar{d}_b H_{3,i,b}\mu_{3,i} + \lambda_b^{*,up}\hat{d}_b H_{3,i,b}\mu_{3,b,i}^{+} \\ &- \lambda_b^{*,dn}\hat{d}_b H_{3,i,b}\mu_{3,b,i}^{-}) + \sum_{t\in\mathcal{T}}\sum_{i=1}^{N_4}\{\Delta\bar{d}_t H_{4,i,t}(\mu_{4,i}^n - \mu_{4,i}^p) \\ &+ \lambda_t^{*,up}\Delta\hat{d}_t H_{4,i,t}(\mu_{4,t,i}^{n,+} - \mu_{4,t,i}^{p,+}) \\ &- \lambda_b^{*,dn}\Delta\hat{d}_t H_{4,i,t}(\mu_{4,t,i}^{n,-} - \mu_{4,t,i}^{p,-})\} + b_5\mu_5 + b_6\mu_6 + b_7\mu_7 \end{aligned}$$

$$\text{s.t.}\quad A_1^T\mu_1 + A_2^T\mu_2 + A_3^T\mu_3 + A_7^T\mu_7 \le 0, \quad (8a)$$

$$A_4^T\mu_4 + A_5^T\mu_5 + A_6^T\mu_6 + A_8^T\mu_7 = 0, \quad (8b)$$

$$-z_b^{\alpha} \le \mu_{2,b,i}^{\kappa,\alpha},\ \mu_{2,i}^{\kappa} \le \mu_{2,b,i}^{\kappa,\alpha} \le 1 - z_b^{\alpha} + \mu_{2,i}^{\kappa}, \quad (8c)$$

$$\forall\kappa \in \{n,p\}, \forall\alpha \in \{+,-\}, \forall b \in \mathcal{B}, \forall i \in \{1,\dots,N_2\},$$

$$-z_b^{\alpha} \le \mu_{3,b,i}^{\alpha},\ \mu_{3,i} \le \mu_{3,b,i}^{\alpha} \le 1 - z_b^{\alpha} + \mu_{3,i}, \quad (8d)$$

$$\forall\alpha \in \{+,-\}, \forall b \in \mathcal{B}, \forall i \in \{1,\dots,N_3\},$$

$$-z_t^{\alpha} \le \mu_{4,t,i}^{\kappa,\alpha},\ \mu_{4,i}^{\kappa} \le \mu_{4,t,i}^{\kappa,\alpha} \le 1 - z_t^{\alpha} + \mu_{4,i}^{\kappa}, \quad (8e)$$

$$\forall\kappa \in \{n,p\}, \forall\alpha \in \{+,-\}, \forall t \in \mathcal{T}, \forall i \in \{1,\dots,N_4\},$$

$$z_b^{+} + z_b^{-} = 1,\ \ z_t^{+} + z_t^{-} = 1, \forall b \in \mathcal{B}, \forall t \in \mathcal{T}, \quad (8f)$$

$$-\mathbf{1} \le \mu_j^{\kappa,\alpha} \le \mathbf{0}, \quad (8g)$$

$$\forall j \in \{2,4\}, \forall\kappa \in \{n,p\}, \forall\alpha \in \{+,-\}$$

$$-\mathbf{1} \le \mu_j^{\alpha} \le \mathbf{0}, \forall j \in \{3\}, \forall\alpha \in \{+,-\}, \quad (8h)$$

$$-\mathbf{1} \le \mu_j \le \mathbf{0}, \forall j \in \{1,3,6,7\} \quad (8i)$$

$$-\mathbf{1} \le \mu_j \le \mathbf{1}, \forall j \in \{2,4,5\},. \quad (8j)$$

If the objective value η^* of subproblem (RDFEA) is greater than 0, we can obtain the following feasibility cut:

$$\begin{aligned}\eta(\lambda) =\ & \sum_{b\in\mathcal{B}}\left(\sum_{i=1}^{N_2}\hat{d}_b H_{2,i,b}(\mu_{2,b,i}^{n+,*} - \mu_{2,b,i}^{p+,*}) + \sum_{i=1}^{N_3}\hat{d}_b H_{3,i,b}\mu_{3,b,i}^{+,*}\right)\lambda_b^{up} \\ &-\sum_{b\in\mathcal{B}}\left(\sum_{i=1}^{N_2}\hat{d}_b H_{2,i,b}(\mu_{2,b,i}^{n-,*} - \mu_{2,b,i}^{p-,*}) + \sum_{i=1}^{N_3}\hat{d}_b H_{3,i,b}\mu_{3,b,i}^{-,*}\right)\lambda_b^{dn} \\ &+ \sum_{t\in\mathcal{T}}\sum_{i=1}^{N_4}\Delta\hat{d}_t H_{4,i,t}(\mu_{4,t,i}^{n+,*} - \mu_{4,t,i}^{p+,*})\lambda_t^{up} \\ &- \sum_{t\in\mathcal{T}}\sum_{i=1}^{N_4}\Delta\hat{d}_t H_{4,i,t}(\mu_{4,t,i}^{n-,*} - \mu_{4,t,i}^{p-,*})\lambda_t^{dn} \\ &+ b_1^T\mu_1^* + \sum_{b\in\mathcal{B}}\sum_{i=1}^{N_2}\bar{d}_b H_{2,i,b}(\mu_{2,i}^{n*} - \mu_{2,i}^{p*}) \\ &+ \sum_{b\in\mathcal{B}}\sum_{i=1}^{N_3}\bar{d}_b H_{3,i,b}\mu_{3,i}^{*} + \sum_{t\in\mathcal{T}}\sum_{i=1}^{N_4}\Delta\bar{d}_t H_{4,i,t}(\mu_{4,i}^{n*} - \mu_{4,i}^{p*}) \\ &+ b_5\mu_5^* + b_6\mu_6^* + b_7\mu_7^* \le 0 \end{aligned} \quad (9)$$

3) Algorithm Framework: We summarize our cutting plan method framework in Fig. 1 as follows:

1) Solve the master problem (MAP) and obtain the optimal solution λ^*.
2) Test the feasibility of the subproblem by solving dual reformulated DFEA problem with λ^*.
3) If the optimal value η^* of DFEA > 0, then update the master problem by adding feasibility cut (9) and go to Step 2. Otherwise, terminate and return the optimal solution and objective value of master problem.

III. Flexibility Indicators

In this section, we propose several flexibility indicators to measure the system flexibility to obtain more information on the system's capability in handling uncertainty. In our problem, we analyze seven different system flexibility indicators: total flexibility (TF), economic dispatch flexibility (EDF), AGC flexibility (AGCF), economic dispatch upward flexibility (EDUPF), economic dispatch downward flexibility (EDDNF), AGC upward flexibility (AGCUPF), and AGC downward flexibility (AGCDNF) based on the simulation results. The definitions of these flexibility indicators are shown in (10a)–(10g).

$$\text{TF} = \frac{\sum_b(\hat{d}_b\lambda_b^{up} + \hat{d}_b\lambda_b^{dn}) + \sum_{t\in\mathcal{T}}(\Delta\hat{d}_t\lambda_t^{up} + \Delta\hat{d}_t\lambda_t^{dn})}{2(\sum_b(\hat{d}_b) + \sum_{t\in\mathcal{T}}(\Delta\hat{d}_t))} \quad (10a)$$

$$\text{EDF} = \frac{\sum_b (\hat{d}_b \lambda_b^{up} + \hat{d}_b \lambda_b^{dn})}{2 \sum_b \hat{d}_b} \tag{10b}$$

$$\text{AGCF} = \frac{\sum_{t \in \mathcal{T}} (\Delta \hat{d}_t \lambda_t^{up} + \Delta \hat{d}_t \lambda_t^{dn})}{2 \sum_{t \in \mathcal{T}} \Delta \hat{d}_t} \tag{10c}$$

$$\text{EDUPF} = \frac{\sum_b (\hat{d}_b \lambda_b^{up})}{\sum_b \hat{d}_b} \tag{10d}$$

$$\text{EDDNF} = \frac{\sum_b (\hat{d}_b \lambda_b^{dn})}{\sum_b \hat{d}_b} \tag{10e}$$

$$\text{AGCUPF} = \frac{\sum_{t \in \mathcal{T}} (\Delta \hat{d}_t \lambda_t^{up})}{\sum_{t \in \mathcal{T}} \Delta \hat{d}_t} \tag{10f}$$

$$\text{AGCDNF} = \frac{\sum_{t \in \mathcal{T}} (\Delta \hat{d}_t \lambda_t^{dn})}{\sum_{t \in \mathcal{T}} \Delta \hat{d}_t} \tag{10g}$$

The TF can gauge both static and dynamic system capability to handle the uncertainty caused by forecasting errors of load and renewable energy resources. The EDF reflects the static capability of the system. The AGCF indicates the capability of the system to respond to the disturbance in real time. The EDUPF and EDDNF can explain up and down static flexibility of the system. The AGCUPF and AGCDNF can describe the up and down dynamic flexibility of the system, respectively.

Notice that all these flexibility indicators are normalized, which means the ranges of these flexibility are in [0, 1]. Let us use the TF to get the insight of the system. When all the λ in the numerator are zero in TF, TF is zero which means the system has no flexibility and cannot handle any uncertainty and disturbance. When all λ in the numerator are 1 in TF, TF is one which means the system can fully response the load change within the uncertainty set. When all λ_b^{up} and λ_b^{dn} are zero, then EDF is zero, which means the system does not have any economic dispatch flexibility. When all λ_b^{up} and λ_b^{dn} are one, then EDF is one, which means the system can achieve its maximum economic dispatch flexibility within the uncertainty set. When all λ_t^{up} and λ_t^{dn} are zero, then AGCF is zero, which means the system does not have any AGC flexibility. When all λ_t^{up} and λ_t^{dn} are one, then AGCF is one, which means the system can achieve its maximum AGC flexibility within the uncertainty set. Similar analysis can be applied to other flexibility indicators.

IV. Case Study

In this section, we test the performance of the proposed flexibility management model with the modified IEEE 118-bus system [29]. These cases are tested by using Julia [30] and CPLEX [31] on Intel Xeon Silver 4216 CPU and 128 G memory.

To get the insights on how the system operators can improve their system flexibility by using limited resources, we investigate on which factors will have impacts on the system flexibility. More specifically, we study key factors including the budget of operational cost, ramping capability, and transmission line capacity.

TABLE I
System Flexibility Under Different Budgets

Budget	SF	TF	EDF	AGCF	EDUPF	EDDNF	AGCUPF	AGCDNF
0	1	0.195	0.207	0.13	0.002	0.413	0.014	0.246
1	1.01	0.271	0.294	0.151	0.176	0.413	0.027	0.275
2	1.05	0.349	0.357	0.31	0.3	0.413	0.272	0.347
3	1.1	0.36	0.357	0.378	0.3	0.413	0.358	0.398
4	1.5	0.383	0.357	0.515	0.3	0.413	0.499	0.531
5	2	0.39	0.357	0.561	0.3	0.413	0.542	0.58
6	2.5	0.391	0.357	0.565	0.3	0.413	0.546	0.585
7	3	0.392	0.357	0.568	0.3	0.413	0.548	0.588
8	4	0.392	0.357	0.574	0.3	0.413	0.552	0.595

In the nominal case, there are 30 units online and the system load is around 86.3% of the total capacity of online units. We assume the uncertain range of the net load at each bus is $[-5\%, 5\%]$ and the system load disturbance is within the range $[-1\%, 1\%]$.

A. Impact of Operational Cost

In this subsection, we first investigate the impact of the operational cost budget by increasing it gradually (denoted from B0 to B8 in Column 1, Table I). We set the budget of the base case (denoted as B0) as the optimal operational cost of the economic dispatch under the nominal foretasted net load. Then we incrementally scale up the budget by using the scale factor (SF) as shown in Column 2 in Table I. For example, the budget of B8 is four times of the budget of B0. All other system parameters are the same in these 9 cases. We report the simulation results of the proposed flexibility indicators under different budgets in Table I.

From Columns 1–5 in Table I, we can observe that three flexibility indicators (i.e., TF, EDF, and AGCF) are non-decreasing as the budget increases. On one hand, for EDF, when the budget is increases by 5% from B0 to B2, the EDF increases significantly for each level of the budget. Once the scale factor (SF) reaches 1.05, EDF remains as a constant number. On the other hand, the AGCF constantly increase until the budget reaches to B5. After that, the AGCF has a very small increase. In addition, we can see that the AGCF is very small when the budget is low. That is because that when the budget is low, EDF will be allocated to more operational cost budget as it has more weight than AGCF in the objective function. But when the system has more budget for operational cost, which is sufficient for the operational cost of the economic dispatch, it will start to allocate budget to the dynamic AGC part. Therefore, with more budget available, AGCF will incur more operational costs. But when the total budget is sufficient for both ED and AGC costs, EDF will not increase and AGC will have very few increments. In addition, the increment of AGCF will result in the increment of TF. We show the trends of indicators TF, EDF, and AGCF in Fig. 2. The Y-axis represents the flexibility indicator values and the X-axis represents the sacle factor. As the flexibility indicators increase, the system has more flexibility.

We further analyze the trend of EDF by looking into its two components: EDUPF and EDDNF, and we show the trends of these three factors in Fig. 3. From the figure, we can observe

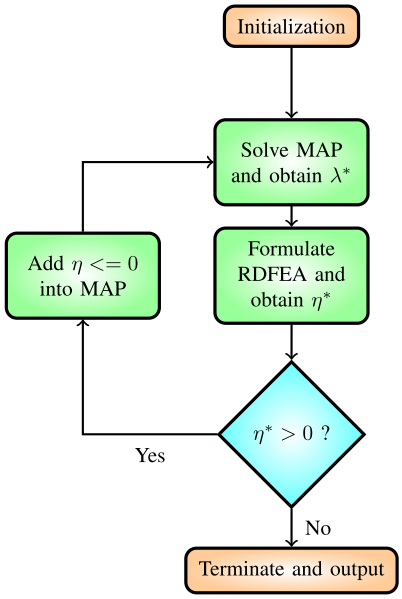

Fig. 1. Flowchart of decomposition algorithm.

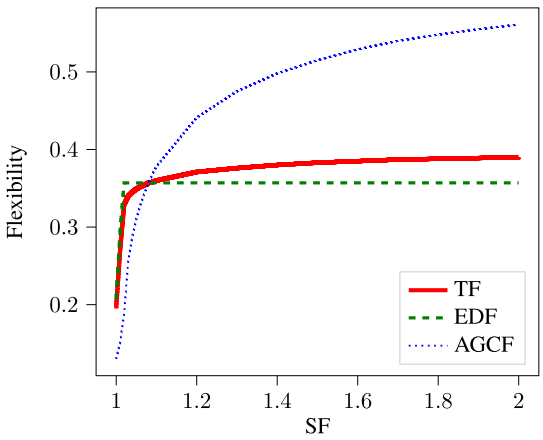

Fig. 2. Trends of TF, EDF, and AGCF.

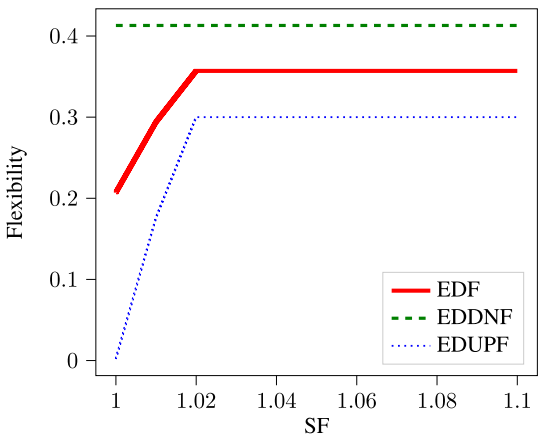

Fig. 3. Trends of EDF, EDUPF, and EDDNF.

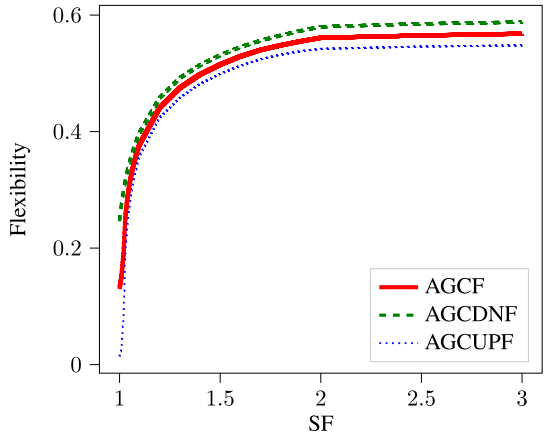

Fig. 4. Trends of AGCF, AGCUPF, and AGCDNF.

TABLE II
SYSTEM FLEXIBILITY UNDER DIFFERENT RAMPING CAPABILITIES

SF	B0			B3			B5		
	TF	EDF	AGCF	TF	EDF	AGCF	TF	EDF	AGCF
1	0.195	0.207	0.130	0.36	0.357	0.378	0.39	0.357	0.541
1.01	0.196	0.208	0.131	0.364	0.361	0.380	0.394	0.361	0.541
1.05	0.199	0.212	0.135	0.374	0.374	0.377	0.402	0.374	0.547
1.1	0.204	0.217	0.140	0.379	0.377	0.389	0.406	0.376	0.558
1.5	0.237	0.249	0.175	0.406	0.401	0.436	0.429	0.399	0.583
2	0.251	0.261	0.200	0.422	0.411	0.483	0.445	0.409	0.624
2.5	0.253	0.261	0.214	0.429	0.411	0.521	0.454	0.41	0.677
3	0.255	0.261	0.222	0.431	0.411	0.537	0.46	0.41	0.712
4	0.257	0.262	0.231	0.432	0.411	0.541	0.467	0.411	0.751

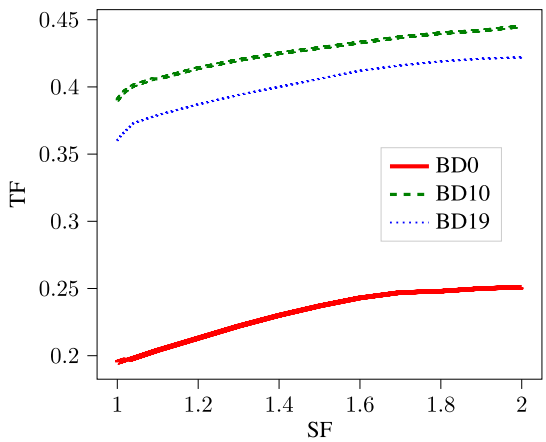

Fig. 5. Trends of TF under different ramping capabilities.

that EDDNF does not change as the budget changes but EDUPF increases and becomes stable when a higher budget is available. That is because the operational cost only includes the fuel cost of thermal units, which means that it can reflect the cost caused by increasing the thermal generators' output. In other words, the economic dispatch upward flexibility can be restricted by the system budget when the system experiences a high load and a low renewable energy output. Therefore, the budget of the operational cost has a significant impact on EDUPF, especially

TABLE III
SYSTEM FLEXIBILITY UNDER DIFFERENT TRANSMISSION LINE CAPABILITIES

SF	B0			B3			B5		
	TF	EDF	AGCF	TF	EDF	AGCF	TF	EDF	AGCF
1	0.195	0.207	0.130	0.36	0.357	0.377	0.39	0.357	0.561
1.01	0.199	0.213	0.130	0.365	0.362	0.377	0.395	0.362	0.561
1.02	0.204	0.218	0.130	0.369	0.368	0.377	0.400	0.368	0.561
1.03	0.208	0.223	0.130	0.373	0.372	0.377	0.403	0.372	0.561
1.04	0.211	0.227	0.130	0.373	0.372	0.377	0.403	0.372	0.561
1.05	0.213	0.229	0.132	0.373	0.372	0.377	0.403	0.372	0.561
1.06	0.213	0.229	0.132	0.373	0.372	0.377	0.403	0.372	0.561
$\geq$ 1.07	0.214	0.229	0.136	0.373	0.372	0.377	0.403	0.372	0.561

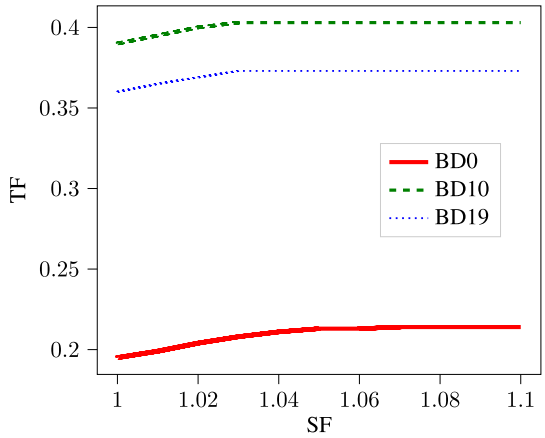

Fig. 6. Trends of TF under different transmission line capabilities.

TABLE IV
COMPUTATIONAL PERFORMANCE

#	Avg (s)	Max (s)	Min (s)
161	8.19	35.78	5.62

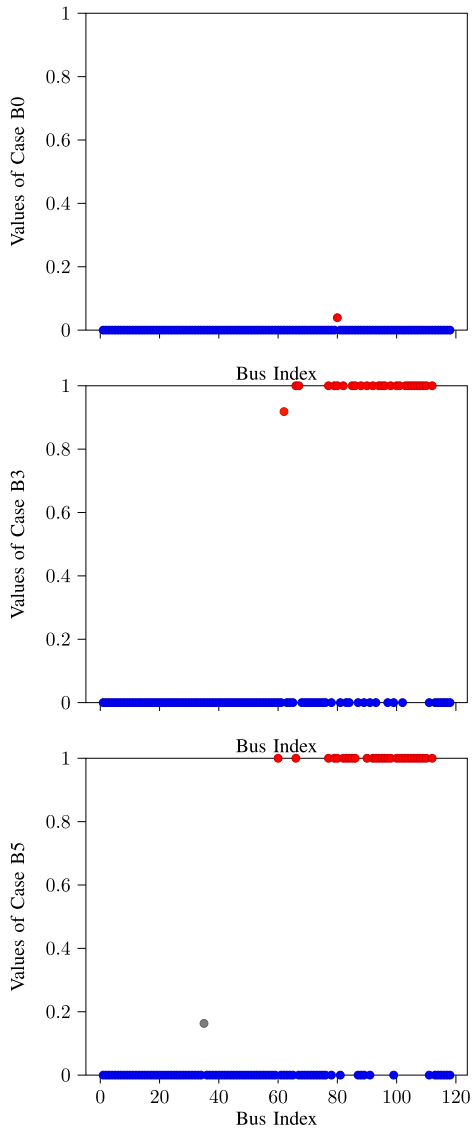

Fig. 7. Optimal value of upper deviation ($\lambda_b^{*,up}$) at each bus.

when the budget is close to the cost of the economic dispatch under nominal case. On the contrary, since there is no cost when generators reduce their output, the budget has little impact on the economic dispatch downward flexibility.

In addition, we show the trends of AGCF, AGCUPF, and AGCDNF in Fig. 4. We can observe that the AGCF is monotonic non-decreasing as the budget increases. Similarly, AGCUPF and AGCDNF both increase monotonic non-decreasing as the budget increases. Because the regulation up/down costs are both limited by the budget constraints, if the budget constraints are related by a larger budget then the AGC units can provide more regulation capability to the system, which means the AGC flexibility indicators can be increased by purchasing more regulation service. Once the scale factor of the budget reaches B5, all flexibility indicators increase slowly.

B. Impacts of Ramping Capability

In this subsection, we report simulation results by increasing the ramping capability of generators under three different budget settings (i.e., B0, B3, and B5). Then, we test different ramping capability settings of all generators in the system to check how flexibility indicators change with ramping capability under a fixed budget. We report flexibility indicators (i.e., TF, EDF, and AGCF) in Table II and show the TF curves in Fig. 5.

Fig. 5 shows that the increasing ramping capability can improve TF of the system. Under all budgets (B0, B3 and B5), the EDF increase until to SF factor reaches to 2.0. After this value, the EDF is almost constant. However, the AGCF has sustained increase as the SF increases under all budget scenarios. From this table, we can observe that the ramp capability can benefit the system flexibility significantly.

C. Impacts of Transmission Line Capacity

In this subsection, we study the impact of transmission line capacity on the system flexibility. Similar to the setup of ramping capability experiments, we study the system flexibility under three different budgets (i.e., B0, B3, and B5). Then we test different scenarios of all the transmission line capacity in Table III by changing the scale factor.

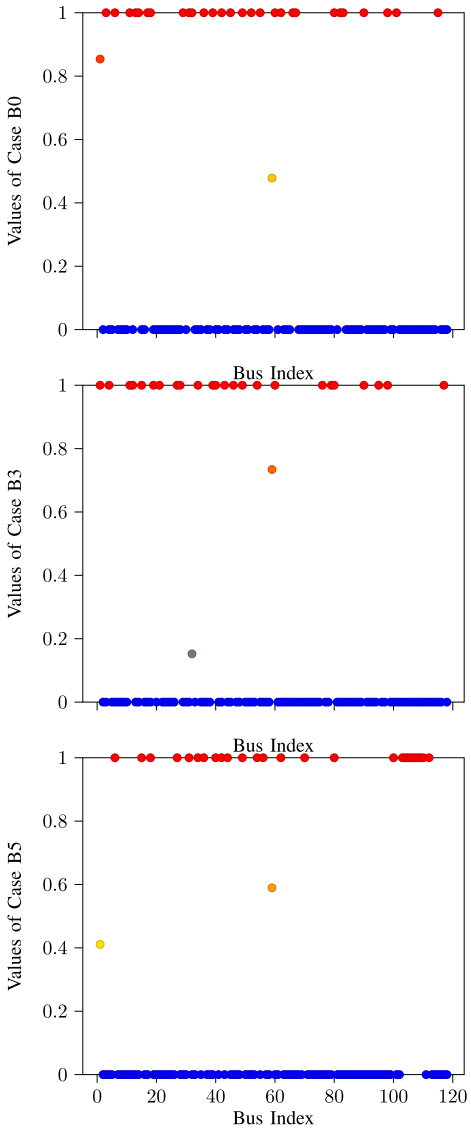

Fig. 8. Optimal Value of Lower Deviation ($\lambda_b^{*,dn}$) at Each Bus.

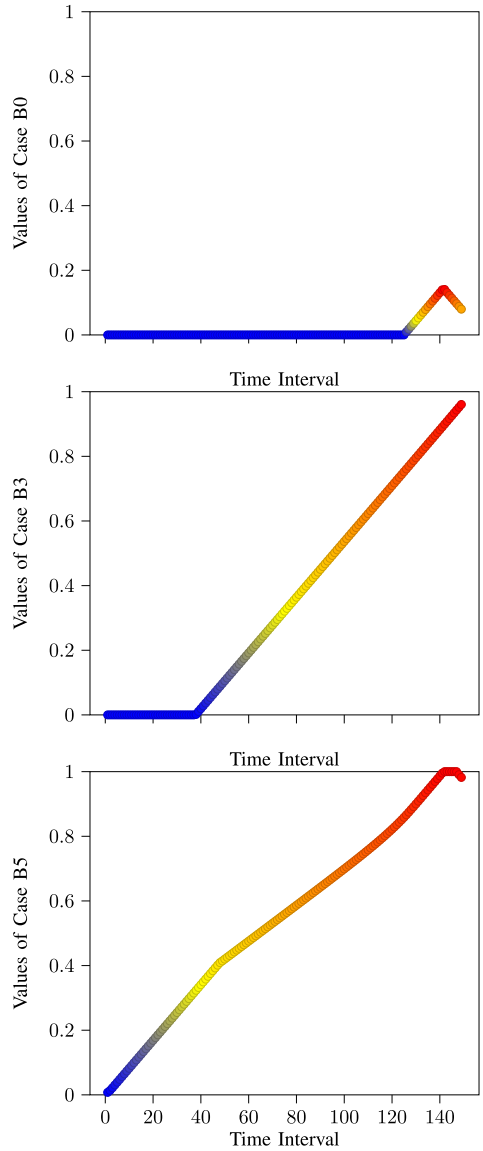

Fig. 9. Optimal Value of Upper Deviation ($\lambda_t^{*,up}$) at Each AGC Interval.

We can observe that under the budget B3 and B5, AGCF remains unchanged, and under budget B0, it changes slightly. This also indicates that improving the transmission capacity has a marginal impact on the AGCF. On the contrary, Fig. 6 demonstrates that a larger transmission line capacity can improve TF for a fixed budget until TF reaches its maximum value. When the scale factor greater than 1.07, the flexibility indicators will not change as shown in the last row of Table III.

D. Computational Performance

In this subsection, we report the statistic information of the computational performance of our algorithm. As shown in the Table IV, we test 161 cases in total. The average computational time is around 8.19 s. The maximum and minimum values are 35.78 s and 5.62 s.

E. Values of Deviations

In this subsection, we report the optimal λ values obtained by the flexibility evaluation model by using scatter plots. In each plot, X-axis represents the bus index and Y-axis represents λ value. The blue points represent the points with the lowest λ value and the red points represent the points with the highest λ value. The color of points will gradually change as the corresponding λ value changes. Fig. 7 and 8 report the optimal values of the upper/lower deviations (i.e., $\lambda_b^{*,up}$, $\lambda_b^{*,dn}$) at each bus of the system under three different budget settings (i.e., B0, B3, and B5). Fig. 9 and 10 report the optimal values of the upper/lower deviations (i.e., $\lambda_t^{*,up}$, $\lambda_t^{*,dn}$) at each AGC cycle (interval) of the system under three different budget settings (i.e., B0, B3, and B5).

From Fig. 7, we can observe that as the budget increases, more buses will allow maximum upper deviations. However, as

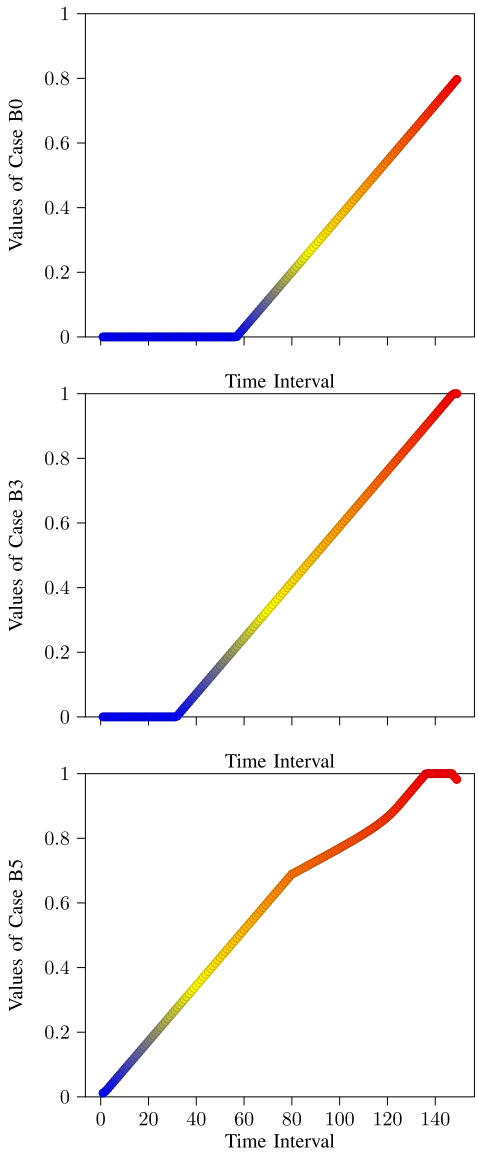

Fig. 10. Optimal Value of Lower Deviation ($\lambda_t^{*,dn}$) at AGC Interval.

shown in Fig. 8, the number of buses that allow maximum lower deviations is not affected too much by the budget. The reason is that under the current setting of the model, no costs occur with the dispatch down actions. From Figs. 9 and 10, we observe that more AGC cycles (intervals) will allow the maximum upper/lower deviations as the budget increases. This verifies that the system can better handle the system load disturbance when the system operational budget is high.

V. Conclusion

In this paper, we proposed a flexibility management framework to model economic dispatch with dynamic AGC constraints. The proposed framework can be solved by conducting reformulation and decomposition. We further proposed seven system flexibility indices (i.e., TF, EDF, AGCF, EDUPF, EDDNF, AGCUPF, AGCDNF) to reflect the system flexibility and studied how the system factors such that the operational cost budget, ramping capacity and transmission line capacity can impact the system flexibility. We found that the budget of the operational cost can significantly contribute to all indicators expect EDDNF, and the improvement of ramping capability can significantly enhance the EDF and the AGCF. In addition, we discover that the transmission capacity only contributes to EDF. As the future work, we will study the power system flexibility with considering the inertia of the resources in the system.

References

[1] U.S. Energy Information Administration Office of Energy Analysis, "Annual Energy Outlook 2020," Washington, DC, USA, January 2020, [Online] Available: https://www.eia.gov/outlooks/aeo/pdf/AEO2020%20Full%20Report.pdf

[2] S. F. Tierney and P. J. Hibbard, "The role and economic impacts of a carbon price in NYISO's wholesale electricity markets," October, 2019, Rensselaer, NY, USA.

[3] CAISO, "SB 100 joint agency report: Charting a path to a 100% clean energy future," 2019. [Online]. Available: https://www.energy.ca.gov/event/workshop/2019-09/joint-agency-workshop-senate-bill-100-report

[4] B. F. Hobbs, J. C. Honious, and J. Bluestein, "What's flexibility worth? the enticing case of natural gas cofiring," *Electricity J.*, vol. 5, no. 2, pp. 37–47, 1992.

[5] E. Ela, M. Milligan, A. Bloom, A. Botterud, A. Townsend, and T. Levin, "Evolution of wholesale electricity market design with increasing levels of renewable generation," Nat. Renewable Energy Lab., Golden, CO, USA, Tech. Rep. NREL/TP-5D00-61765, 2014.

[6] E. Lannoye, D. Flynn, and M. O'Malley, "Evaluation of power system flexibility," *IEEE Trans. Power Syst.*, vol. 27, no. 2, pp. 922–931, May 2012.

[7] M. A. Bucher, S. Delikaraoglou, K. Heussen, P. Pinson, and G. Andersson, "On quantification of flexibility in power systems," in *Proc. IEEE Eindhoven PowerTech*, 2015, pp. 1–6.

[8] Q. Wang and B.-M. Hodge, "Enhancing power system operational flexibility with flexible ramping products: A review," *IEEE Trans. Ind. Informat.*, vol. 13, no. 4, pp. 1652–1664, Aug. 2017.

[9] C. Liu and P. Du, "Participation of load resources in day-ahead market to provide primary-frequency response reserve," *IEEE Trans. Power Syst.*, vol. 33, no. 5, pp. 5041–5051, Sep. 2018.

[10] F. Wang, A. Korad, and Y. Chen, "Reserve deliverability with application to short-term reserve product," in *Proc. FERC Tech. Conf. Increas. Real-Time Day-Ahead Market Efficiency. Through Improved Softw.*, Washington DC, USA, Jun. 2019.

[11] L. Fan and Y. Guan, "An edge-based formulation for combined-cycle units," *IEEE Trans. Power Syst.*, vol. 31, no. 3, pp. 1809–1819, May 2016.

[12] C. Dai, Y. Chen, F. Wang, J. Wan, and L. Wu, "A configuration-component-based hybrid model for combined-cycle units in MISO day-ahead market," *IEEE Trans. Power Syst.*, vol. 34, no. 2, pp. 883–896, Mar. 2019.

[13] J. Garcia-Gonzalez, R. M. R. de la Muela, L. M. Santos, and A. M. Gonzalez, "Stochastic joint optimization of wind generation and pumped-storage units in an electricity market," *IEEE Trans. Power Syst.*, vol. 23, no. 2, pp. 460–468, May 2008.

[14] T. Ding *et al.*, "Rectangle packing problem for battery charging dispatch considering uninterrupted discrete charging rate," *IEEE Trans. Power Syst.*, vol. 34, no. 3, pp. 2472–2475, May 2019.

[15] B. Xu, J. Zhao, T. Zheng, E. Litvinov, and D. S. Kirschen, "Factoring the cycle aging cost of batteries participating in electricity markets," *IEEE Trans. Power Syst.*, vol. 33, no. 2, pp. 2248–2259, Mar. 2018.

[16] Y. Guan, L. Fan, and Y. Yu, "Unified formulations for combined-cycle units," *IEEE Trans. Power Syst.*, vol. 33, no. 6, pp. 7288–7291, Nov. 2018.

[17] S. Babaei, C. Zhao, and L. Fan, "A data-driven model of virtual power plants in day-ahead unit commitment," *IEEE Trans. Power Syst.*, vol. 34, no. 6, pp. 5125–5135, Nov. 2019.

[18] X. Chen, E. Dall'Anese, C. Zhao, and N. Li, "Aggregate power flexibility in unbalanced distribution systems," *IEEE Trans. Smart Grid*, vol. 11, no. 1, pp. 258–269, Jan. 2020.

[19] J. Zhao, T. Zheng, and E. Litvinov, "A unified framework for defining and measuring flexibility in power system," *IEEE Trans. Power Syst.*, vol. 31, no. 1, pp. 339–347, Jan. 2016.

[20] D. Bertsimas, E. Litvinov, X. A. Sun, J. Zhao, and T. Zheng, "Adaptive robust optimization for the security constrained unit commitment problem," *IEEE Trans. Power Syst.*, vol. 28, no. 1, pp. 52–63, Feb. 2013.
[21] R. Jiang, J. Wang, and Y. Guan, "Robust unit commitment with wind power and pumped storage hydro," *IEEE Trans. Power Syst.*, vol. 27, no. 2, pp. 800–810, May 2012.
[22] Y. An and B. Zeng, "Exploring the modeling capacity of two-stage robust optimization: Variants of robust unit commitment model," *IEEE Trans. Power Syst.*, vol. 30, no. 1, pp. 109–122, Jan. 2015.
[23] G. Zhang, "New ancillary service market design to improve MW-frequency performance: reserve adequacy and resource flexibility," PhD Dissertation, 2015, ISU, Ames, IA, USA.
[24] X. Xia and A. Elaiw, "Optimal dynamic economic dispatch of generation: A review," *Electric Power Syst. Res.*, vol. 80, no. 8, pp. 975–986, 2010.
[25] A. Lorca and X. A. Sun, "Adaptive robust optimization with dynamic uncertainty sets for multi-period economic dispatch under significant wind," *IEEE Trans. Power Syst.*, vol. 30, no. 4, pp. 1702–1713, Jul. 2015.
[26] W. Li and Y. Chen, "MISO AGC enhancement proposal to better utilize fast ramping resources," in *Proc. IEEE Power Energy Soc. Gen. Meeting*, 2015, pp. 1–5.
[27] G. Zhang, J. McCalley, and Q. Wang, "An AGC dynamics-constrained economic dispatch model," *IEEE Trans. Power Syst.*, vol. 34, no. 5, pp. 3931–3940, Sep. 2019.
[28] L. Fan, J. Wang, R. Jiang, and Y. Guan, "Min-max regret bidding strategy for thermal generator considering price uncertainty," *IEEE Trans. Power Syst.*, vol. 29, no. 5, pp. 2169–2179, Sep. 2014.
[29] "IEEE 118-bus system," [Online]. Available: https://github.com/LFPower/IEEE-118Bus-System
[30] M. Lubin and I. Dunning, "Computing in operations research using Julia," *Informs J. Comput.*, vol. 27, no. 2, pp. 238–248, 2015.
[31] IBM, "IBM CPLEXoptimizer," [Online]. Available: https://www.ibm.com/analytics/cplex-optimizer

Lei Fan (Senior Member, IEEE) received the Ph.D. degree in operations research from Industrial and System Engineering Department, University of Florida, Gainesville, FL, USA. He is currently an Assistant Professor with the Engineering Technology Department, University of Houston, Houston, TX, USA. Before this position, he was with the electricity energy industry for various years. His research interests include optimization methods, complex system operations, and power system operations and planning.

Chaoyue Zhao (Member, IEEE) received the B.S. degree in information and computing sciences from Fudan University, Shanghai, China, in 2010, and the Ph.D. degree in industrial and systems engineering from the University of Florida, Gainesville, FL, USA, in 2014. She is currently an Assistant Professor of industrial and systems engineering with the University of Washington, Seattle, WA, USA and previously was an Assistant Professor of industrial engineering and management with Oklahoma State University, Stillwater, OK, USA. In 2013, she was with the Pacific Gas and Electric Company. Her research interests include distributionally robust optimization and reinforcement learning with their applications in power system scheduling, planning, and resilience.

Guangyuan Zhang (Member, IEEE) received the B.S. degree from Xi'an Jiaotong University, Xi'an, China, in 2008, the M.S. degree from the Illinois Institute of Technology, Chicago, IL, USA, in 2011, and the Ph.D. degree from Iowa State University, Ames, IA, USA, in 2015. He is currently the Senior Commercial Analyst with RWE Renewables America. His research interests include power system optimization and power market operations.

Qiuhua Huang (Member, IEEE) received the B.Eng. and M.Eng. degrees in electrical engineering from the South China University of Technology, Guangzhou, China, in 2009 and 2012, respectively, and the Ph.D. degree in electrical engineering from Arizona State University, Tempe, AZ, USA, in 2016. He is currently a Senior Power System Research Engineer in the Electricity Security Group, Pacific Northwest National Laboratory. His research interests include power transmission and distribution systems modeling, simulation and control, and application of machine learning and advanced computing technologies in power and energy systems. He was the recipient of the 2019 IEEE PES Prize Paper Award and 2018 R & D 100 Award, and two IEEE PES General Meeting best paper awards. He is an Associate Editor for the *CSEE Journal of Power and Energy Systems*, and IEEE ACCESS.